Geochemistry International, Vol. 42, No. 6, 2004, pp. 497–512. Translated from Geokhimiya, No. 6, 2004, pp. 579–596.

Compositions and Formation Conditions of Silicate and Salt Magmas Forming the Garnet Syenite Porphyries (Sviatonossites) of the Carbonatite-Bearing Mushugai-Khuduk Complex, Southern Mongolia

I. A. Andreeva*, V. I. Kovalenko*, V. B. Naumov, and N. N. Kononkova****

**Institute of Geology of Ore Deposits, Petrography, Mineralogy, and Geochemistry (IGEM), Russian Academy of Sciences, Staromonetnyi per. 35, Moscow, 119017 Russia*
e-mail: andreeva@igem.ru
***Vernadsky Institute of Geochemistry and Analytical Chemistry, Russian Academy of Sciences, ul. Kosygina 19, Moscow, 119991 Russia*
e-mail: naumov@geokhi.ru
Received July 15, 2003

Abstract—Crystalline and melt inclusions were studied in garnet, diopside, potassium feldspar, and sphene from the garnet syenite porphyry (sviatonossite) of the Mushugai-Khuduk carbonatite-bearing complex in southern Mongolia. Phlogopite, clinopyroxene, albite, potassium feldspar, sphene, wollastonite, magnetite, Ca and Sr sulfates, calcite, fluorite, and apatite were identified among the crystalline inclusions. The melt inclusions were analyzed on an electron microprobe. They were represented by silicate and salt melts and showed homogenization temperatures of 1010–1080°C. Silicate melt inclusions were found in diopside, potassium feldspar, and sphene. They had a variable SiO_2 content, from 56 to 66 wt %, and showed high $Na_2O + K_2O$ (up to 17 wt %), Zr, F, and Cl concentrations. In general the silicate melts were chemically similar to alkali syenite. Salt melt inclusions were found in diopside and garnet. In the course of thermometric experiments, they produced homogeneous quench glasses of sulfate-dominated compositions with an SiO_2 content no higher than 1.3 wt %. These melts are strongly enriched in Ba, Sr, P, F, and Cl. The investigation of the silicate and salt melt inclusions provided evidence for the magmatic genesis of the sviatonossites. These rocks were formed under the influence of the processes of crystallization differentiation and magma separation into immiscible silicate and salt (sulfate) liquids.

INTRODUCTION

Alkaline igneous complexes with carbonatites have been the focus of extensive geological and petrological studies. It is well known that carbonatite-bearing complexes accumulate a variety of rare and ore components (REE, Nb, Ta, P, U, Th, Ba, Sr, Pb, Zn, etc.) often reaching economic levels. In this context, the compositions of ore-generating magmas and the processes of ore component enrichment in magmatic systems controlling the formation of mineral deposits remain as urgent scientific issues. During the past decades, these topics have been addressed by various authors by the examples of the alkaline carbonatite-bearing complexes of the Kola Peninsula, eastern Pamirs, Aldan, southern Africa, etc. [1–5]. Our previous investigations of the Late Mesozoic potassium alkaline carbonatite-bearing complex Mushugai-Khuduk in southern Mongolia demonstrated that the alkaline and ore-bearing rocks of this complex were formed from silicate, silicate–salt (silicate–phosphate), and salt melts of various geochemical signatures (carbonate–phosphate, phosphate–sulfate, fluoride–sulfate, chloride–sulfate, etc.). It was shown that salt components played a key role in the accumulation of ore elements in silicate magmatic melts up to the formation of economic concentrations [6–10].

Here we report the results of a study of melt inclusions in the minerals of ore-bearing garnet syenite porphyries, which were found during test drilling operations in the region of the Mushugai deposit. These are unique rocks containing garnet crystals up to 5–6 cm across in a fine-grained syenite mesostasis. The nature of these rocks (magmatic or metasomatic) is still a matter of debate. The use of modern methods of melt inclusion investigation allowed us to resolve this dilemma. We estimated the physicochemical parameters and compositions of mineral-forming media for these rocks and determined the processes that were responsible for their formation.

GEOLOGICAL BACKGROUND

The geologic setting of the Mushugai-Khuduk complex was described in detail by Samoĭlov and Kovalenko [11]. The rocks of this complex were formed at shallow (volcanic and subvolcanic) levels. They intruded a Paleozoic stratified volcanosedimentary sequence and were overlain by Early Cretaceous

basalts. Their age is between the Late Jurassic and the Early Cretaceous. The complex is built up of diverse alkaline extrusive (including pyroclastic), subvolcanic, and intrusive alkaline and subalkaline rocks ranging in composition from melanephelinite and nepheline melaleucitite to trachydacite and latite in the extrusive facies, and from shonkinite to quartz syenite and rhyolite in the plutonic facies. The alkaline magmatism is spatially and genetically linked with the formation of ore mineralization in the complex, including mineralized breccias with a carbonate cement, carbonatite, and apatite-rich rocks. Test and assessment drilling operations were performed in some of the areas of the Mushugai ore occurrence that showed the highest abundance of mineralized rocks. Some boreholes were drilled to depths of 70–300 m. This activity revealed rare earth ores of various geochemical types. Some of them were previously described on the surface, others were first found in drill cores. In general, there are two main types of ores: (1) carbonatitic and (2) apatite-bearing ores.

The carbonatitic type includes (a) mineralized breccias forming relatively large, usually steeply dipping mineralized zone; and (b) carbonatite-series rocks composing mainly vein and stockwork bodies. The mineralized breccias are usually closely associated with the carbonatite-series rocks and often sit in the same pyroclastic units. The mineralogical and chemical compositions of the mineralized breccias depend, on the one hand, on the proportions of clasts and cement and, on the other hand, on the composition of the cement. Their clastic material is usually represented by syenite, syenite porphyry, trachyte, occasional trachyrhyodacite, and other alkaline rocks. The exploration of the chemical and mineralogical composition of the mineralized breccias showed that TiO_2, Al_2O_3, MnO, MgO, Na_2O, K_2O, P_2O_5, and, in part, SiO_2 are accumulated mainly in the breccia clasts, whereas the cement concentrates CaO, SrO, BaO, Fe_2O_3, REE, and volatile components. The mineralized breccias are often enriched in lead (up to 1.1 wt % PbO).

The composition of carbonatite-series rocks varies considerably owing to variations in the proportions of carbonate, fluorite, and quartz. There are continuous series from carbonatite proper to fluorite-dominated and siliceous rocks. The lowest REE concentrations were measured in the silica-rich rocks and some carbonatite varieties, the highest concentrations were confined to the fluorite-bearing varieties (fluorite carbonatite, carbonate–fluorite, siliceous fluorite, and other rocks). Strontium resides primarily in celestite, and barium, in barite. The area of the Mushugai ore occurrence comprises approximately equal amounts of carbonatites proper and other members of the carbonatite association, such as magnetite–apatite, fluorite, celestite–fluorite, and other rocks.

The apatite-bearing REE ores include (a) magnetite–apatite rocks forming veins, stockworks, and bodies of mineralized breccias; (b) apatite and phlogopite–apatite rocks; (c) feldspar–apatite rocks; and (d) alkaline rocks (syenite, syenite porphyry, etc.) containing abundant apatite and garnet megacrysts and schlieren of apatite-dominated rocks. Apatite is the main repository for REE (up to 9.5 wt %) in all the types of apatite-bearing rocks.

Thus, the results of test and assessment drilling allow us to conclude that REE mineralization is widespread and extends to deep levels. The Mushugai ores, both from surface exposures and recovered by drilling, show high concentrations of REE, primarily of the light REE lanthanum, cerium, and neodymium. However, high-grade REE ores may also be enriched in other lanthanides (e.g., europium and samarium) and yttrium. The ores, especially apatite-bearing ones, are multielemental and are simultaneously enriched in REE, strontium, and barium.

CHARACTERISTICS OF THE SAMPLE STUDIED

Garnet syenite porphyry was recovered by drilling in a large (~30–70 m) stockwork-like apatite body in the eastern part of the complex [11]. It is a light gray rock containing large garnet crystals up to 5–6 cm across embedded in a fine-grained syenitic mesostasis. The phenocrysts assemblage of the syenite is dominated by potassium feldspar (~40–45%), diopside (~15–20%), and plagioclase (~5–10%). Secondary and accessory minerals include sphene, phlogopite, zircon, apatite, magnetite, ilmenite, and pyrite. It is remarkable that calcite, celestite, and fluorite occur as accessory minerals (Table 1).

Large garnet phenocrysts have a dark brown color and distinct crystal faces. Their chemical compositions correspond to the andradite–grossular solid solution with high TiO_2 (up to 4 wt %) (Table 1, an. 9). The garnet is usually surrounded by a reaction rim composed of small grains of garnet, diopside, sphene, and potassium feldspar. It is noteworthy that the garnet from the reaction rim has an andradite composition (Table 1, an. 10) and contains up to 5 wt % TiO_2. Rock-forming andradite was previously reported from the nepheline syenites of East Greenland and Iivaara [12].

Diopside and plagioclase are distinctly more euhedral than potassium feldspar. Diopside forms elongated prismatic crystals, from 0.3 to 1.0 mm in size. Diopside is sometimes replaced by amphibole. The prismatic plagioclase crystals are 1–2 mm in size. Their compositions correspond to oligoclase and albite (Table 1, an. 4 and 5).

The crystals of potassium feldspar often show perthitic textures. They contain inclusions of clinopyroxene, sphene, fluorite, and magnetite. Among the characteristic features of their chemical composition are high BaO (up to 0.8 wt %) and SrO (up to 1.1 wt %) concentrations (Table 1, an. 6).

Sphene and apatite are the most common minor and accessory phases. Sphene occurs as light yellow

Table 1. Chemical compositions (wt %) of the garnet-bearing syenite porphyry and its minerals

Component	1	2	3	4	5	6	7	8	9	10	11	12	13	14	15	16	17	18
SiO_2	43.35	49.72	39.51	63.19	65.90	65.30	30.01	29.79	36.00	34.44	36.45	0.92	7.33	0.14	0.12	2.27	0.05	0.11
TiO_2	1.10	0.39	4.82	0.02	0.07	0.04	32.06	31.75	3.95	4.81	0.00	0.00	0.01	0.04	0.00	0.00	48.19	0.00
Al_2O_3	11.35	1.68	14.69	25.20	19.97	20.46	1.12	1.47	10.57	3.63	0.05	0.05	0.10	0.03	0.04	0.84	0.13	0.00
FeO	7.61	15.80	10.19	0.68	1.24	0.14	2.16	2.29	14.71	21.92	0.00	0.30	0.02	0.11	0.00	92.51	42.14	47.97**
MnO	0.18	0.45	0.14	0.02	0.01	0.00	0.07	0.00	0.27	0.16	0.01	0.00	0.00	0.46	0.02	0.16	2.95	0.00
MgO	0.45	7.39	17.95	0.14	1.00	0.00	0.00	0.03	0.62	0.39	0.09	0.00	0.02	0.00	0.00	0.19	2.35	0.03
BaO	0.31	0.00	1.14	–	–	0.00	0.67	0.58	0.04	–	0.03	0.07	0.00	0.05	0.53	–	–	–
SrO	1.22	0.00	–	–	–	0.00	–	–	0.00	–	0.00	0.64	0.10	0.22	54.98	–	–	–
CaO	18.56	23.10	0.00	5.73	0.33	0.14	26.50	26.32	34.32	32.15	0.01	53.33	47.75	57.90	0.14	0.52	0.02	0.01
Na_2O	3.61	0.86	0.42	6.31	10.58	0.91	0.07	0.03	0.00	0.06	0.00	0.33	0.32	0.00	0.05	0.21	0.03	0.05
K_2O	2.22	0.02	8.71	0.27	0.96	13.88	0.05	0.01	0.00	0.08	0.03	0.01	0.10	0.02	0.04	0.13	0.00	0.02
P_2O_5	1.34	0.00	0.00	0.00	0.00	0.00	0.00	0.00	0.00	–	0.00	39.63	27.02	0.02	–	–	–	–
Ce_2O_3	–	0.00	0.39	–	–	0.00	1.25	1.51	0.01	–	0.10	0.63	5.21	0.00	0.00	–	–	–
La_2O_3	–	0.00	0.04	–	–	0.00	0.24	0.54	0.00	–	0.00	0.27	2.61	0.00	0.00	–	–	–
ZrO_2	–	–	0.00	–	–	0.00	2.13	2.86	–	–	64.44	–	–	–	–	–	–	–
Nb_2O_5	–	–	0.02	–	–	–	1.18	0.66	–	–	0.00	–	–	–	–	–	–	–
Nd_2O_3	–	–	0.00	–	–	–	0.69	0.49	–	–	0.06	–	–	–	–	–	–	–
F	0.27	0.02	0.37	–	–	–	0.24	0.00	–	–	0.00	3.97	2.88	0.08	–	–	–	–
Cl	0.00	0.01	0.01	0.02	0.00	0.01	0.05	0.01	0.00	0.00	0.02	0.01	0.00	0.00	0.00	0.07	0.02	0.03
S	0.43	0.00	0.02	0.01	0.00	0.00	0.01	0.00	0.01	0.01	0.00	0.30	0.90	0.00	44.18*	0.12	0.00	51.91
Total	100.40	99.44	98.42	101.59	100.06	100.88	98.50	98.34	100.50	97.65	101.29	100.46	94.37	59.07	100.10	97.02	95.88	100.13

Note: Here and in other tables, FeO is total iron recalculated as FeO. 1, Rock; total includes 1.91 wt % H_2O, 3.87 wt % CO_2, and 1.62 wt % REE; 2, diopside; 3, phlogopite; 4, oligoclase; 5, albite; 6, potassium feldspar; 7 and 8, sphene; 9 and 10, garnet; 11, zircon; 12 and 13, F-apatite; 14, calcite; 15, celestite; 16, magnetite; 17, ilmenite; and 18, pyrite.

* Concentration of SO_3.

** Concentration of Fe.

wedge-shaped crystals, up to 0.8 mm in size, often associating with diopside and plagioclase. It shows high concentrations of Zr_2O_3 (up to 2.9 wt %), Ce_2O_3 + La_2O_3 (up to 2 wt %), Nb_2O_5 (from 0.7 to 1.2 wt %), Nd_2O_3 (up to 0.7 wt %), and BaO (up to 0.7 wt %) (Table 1, an. 7 and 8). Sphene of similar composition was previously reported by Andreeva *et al.* [9] from the theralite of the same complex.

Apatite forms relatively small euhedral crystals, sometimes intergrown with diopside, and larger grains composing aggregates within potassium feldspar. In addition, apatite occurs in association with fine-grained calcite, which sometimes forms segregations up to 2 mm in size. Its composition corresponds to a fluorapatite (2.9–4.0 wt % F) with elevated concentrations of SrO (up to 0.64 wt %), Ce_2O_3 + La_2O_3 (up to 1 wt %), and S (up to 0.3 wt %) (Table 1, an. 12). Of particular interest is the occurrence of a phosphate mineral transitional between apatite and britholite (Table 1, an. 13) in the rock together with fluorapatite. This phase is characterized by high concentrations of Ce_2O_3 and La_2O_3 (comprising together up to 8 wt %) and sulfur (up to 0.9 wt %). It contains 27 wt % P_2O_5 and 7 wt % SiO_2.

Phlogopite is rather scarce and forms flakes up to 0.5 mm in size. It is rich in TiO_2 (up to 5 wt %) and BaO (up to 1.1 wt %). Zircon, celestite, and fluorite occur as small crystals usually included in potassium feldspar.

The opaque minerals of the rock are magnetite, ilmenite, and pyrite. They occur as irregular grains in potassium feldspar, often in association with celestite and apatite.

The groundmass of the garnet-bearing syenite porphyry is composed mainly of potassium feldspar and plagioclase. Small opaque mineral grains occur in minor amounts. Potassium feldspar forms small crystals (up to 0.1–0.2 mm) in the groundmass, often with perthitic textures. Plagioclase occurs as tabular crystals of albitic composition.

In general, the mineralogical and chemical compositions of the rock studied are similar to those of sviatonossite, a rare variety of garnet syenite first discovered and described by Escola in 1921 [13].

STUDY METHODS

Inclusions in minerals were initially inspected in polished sections, 0.3 mm thick. Thermometric investigations were carried out in electric furnaces and a Linkam TS 1500 microscopic heating stage allowing visual control during high-temperature experiments. The error of temperature measurement was ±10°C. In order to approach equilibrium between melt and the host mineral, the samples were kept at the desired temperature for 30 min in an electric furnace.

The compositions of glasses of homogenized melt inclusions, daughter phases in the inclusions, crystalline inclusions, and rock-forming minerals were determined by X-ray spectral electron probe microanalysis (EPMA). Analyses were obtained at an accelerating voltage of 15 kV and a beam current of 30 nA. The glasses of melt inclusions were analyzed by scanning over areas of 12×12, 5×5 or 2×2 μm. Daughter mineral phases in inclusions and crystalline inclusions were analyzed either in a point with a focused beam or by scanning over areas of 5×5 and 2×2 μm. Rock-forming minerals were analyzed by scanning over an area of 5×5 μm.

RESULTS OF INCLUSION STUDY

Primary magmatic inclusions were found and studied in diopside, sphene, potassium feldspar, and garnet from the garnet syenite porphyry. Based on their phase composition, they are grouped into crystalline and melt inclusions. It is noteworthy that very few data on melt inclusions in garnet are available [14–16].

Crystalline Inclusions

Diverse mineral inclusions occur in diopside, potassium feldspar, and garnet. There are both silicate and nonsilicate phases: phlogopite, clinopyroxene, albite, potassium feldspar, sphene, wollastonite, magnetite, gypsum, celestite, calcite, fluorite, apatite, and a phosphate mineral of the apatite group. The compositions of the crystalline inclusions are listed in Table 2.

Phlogopite inclusions were found in diopside as platy dark brown crystals, up to 50 μm in size. They are rich in TiO_2 (4.7 wt %) and F (up to 5 wt %). The phlogopite of the rock is characterized by a much lower F concentration, no higher than 0.4 wt %. Clinopyroxene inclusions of diopside composition were found in potassium feldspar and garnet. They were prismatic light green crystals, up to 40 μm in size. The clinopyroxene was enriched in MnO (up to 0.5 wt %).

Sphene crystalline inclusions were found in diopside and potassium feldspar. They were wedge-shaped crystals of light yellow color, from 30 to 50 μm in size. Similar to accessory sphene in the rock groundmass, sphene inclusions are rich in ZrO_2 (3.5–4.2 wt %) and rare earth elements (up to 2.5 wt % Ce_2O_3 + La_2O_3).

Inclusions of potassium feldspar were encountered in diopside and garnet. The inclusions are prismatic and vary in size from 30 to 60 μm. Their BaO and SrO contents were relatively low, 0.30 and 0.24 wt %, respectively. Albite is very rare among crystalline inclusions and was found in diopside only. In addition to albite, diopside bears opaque mineral inclusions. They were rounded in shape and from 20 to 40 μm in size. The composition of these inclusions corresponds to a magnetite with no more than 0.8 wt % TiO_2.

The phosphate and carbonate minerals apatite and calcite are also rather common as crystalline inclusions in diopside and garnet. Apatite forms euhedral colorless crystals of prismatic habit, from 25 to 50 μm in size. It

Table 2. Chemical compositions (wt %) of crystalline inclusions in the minerals of the garnet-bearing syenite porphyry

Component	1	2	3	4	5	6	7	8	9	10	11	12	13	14	15	16	17	18
SiO_2	48.00	47.94	38.00	64.16	62.03	67.20	30.39	29.59	30.35	1.98	10.78	1.94	0.75	0.40	51.58	0.55	0.34	0.14
TiO_2	0.38	1.16	4.70	0.03	0.05	0.03	33.35	35.46	32.04	0.25	0.04	0.81	0.01	0.05	0.11	0.05	0.72	0.00
Al_2O_3	3.94	3.05	13.45	19.14	18.45	19.64	1.58	1.20	1.50	0.14	0.15	1.32	0.04	0.10	0.15	0.20	0.06	0.23
FeO	16.82	14.61	12.45	0.28	0.64	0.91	3.58	1.82	2.57	0.77	0.58	93.24	0.79	0.50	0.62	0.55	0.25	0.06
MnO	0.48	0.38	0.27	0.00	0.00	0.06	0.00	0.04	0.00	0.00	0.09	0.04	0.01	0.09	0.16	0.08	0.06	0.02
MgO	7.21	7.99	14.72	0.01	0.27	0.10	0.15	0.05	0.02	0.24	0.00	0.43	0.19	0.00	0.21	0.00	0.04	0.00
CaO	22.11	21.61	0.39	0.43	0.64	0.64	25.12	26.10	24.92	51.20	46.64	0.92	61.51	62.13	47.52	39.57	0.86	56.21
BaO	0.09	0.05	0.24	–	0.30	0.00	0.19	0.62	0.34	–	0.07	–	–	0.00	0.00	0.00	1.24	0.07
SrO	0.04	0.00	0.29	–	0.24	0.00	0.00	0.03	0.21	–	0.44	–	–	0.14	0.07	1.52	69.60	0.00*
Na_2O	1.50	1.07	0.90	1.46	3.11	10.48	0.00	0.00	0.02	0.61	0.12	0.18	0.07	0.01	0.00	0.02	0.08	0.07
K_2O	0.01	0.14	11.13	15.19	14.12	1.45	0.02	0.00	0.32	0.13	0.00	0.57	0.01	0.00	0.02	0.12	0.01	0.28
P_2O_5	0.00	0.00	0.00	0.01	0.00	0.01	0.00	0.02	0.01	40.99	20.70	0.01	0.00	0.09	0.02	0.01	0.00	0.00
Ce_2O_3	0.00	0.00	0.10	–	0.17	0.00	0.84	1.34	1.93	0.87	6.93	–	–	0.00	0.00	0.02	0.58	0.03
La_2O_3	0.00	0.00	0.01	–	0.00	0.00	0.28	0.34	0.55	0.43	2.74	–	–	0.06	0.00	0.00	0.06	0.01
ZrO_2	0.00	0.15	0.01	–	0.08	0.00	4.24	3.67	3.43	–	–	–	–	–	–	–	0.00	0.00
F	0.05	0.00	4.91	–	0.48	0.00	0.80	0.20	0.53	3.01	2.73	–	0.00	0.01	0.01	0.07	0.00	42.28
Cl	0.00	0.00	0.01	0.02	0.00	0.03	0.00	0.00	0.00	0.04	0.25	0.01	0.02	0.06	0.00	0.18	0.01	0.01
S	0.00	0.00	0.03	0.00	0.10	0.00	0.01	0.01	0.02	0.33	2.78	0.03	0.01	0.00	0.00	47.45*	26.4*	0.01
Total	100.63	98.15	101.62	100.75	100.68	100.54	100.56	100.49	98.75	100.98	100.31	99.50	63.44	63.64	100.47	90.39	100.31	99.43
Host minerals	*Grt*	*Kfs*	*Di*	*Grt*	*Di*	*Di*	*Di*	*Di*	*Kfs*	*Di*	*Grt*	*Di*	*Di*	*Grt*	*Grt*	*Grt*	*Sph*	*Kfs*

Note: Host minerals: *Grt*, garnet; *Kfs*, potassium feldspar; *Di*, diopside; and *Sph*, sphene. 1 and 2, diopside; 3, phlogopite; 4 and 5, potassium feldspar; 6, albite; 7–9, sphene; 10, apatite; 11, phosphate, total includes 0.23 wt % UO_2, 2.41 wt % ThO_2, 1.71 wt % Nd_2O_3, and 0.92 wt % Sm_2O_3; 12, magnetite; 13 and 14, calcite; 15, wollastonite; 16, gypsum; 17, celestite; and 18, fluorite.

*Concentration of SO_3.

Table 3. Chemical compositions (wt %) of the daughter minerals and glasses of homogenized melt inclusions in diopside from the garnet-bearing syenite porphyry

Component	1	2	3	4	5	6	7	8	9	10	11
SiO_2	54.50	0.05	56.66	57.91	59.95	58.90	61.33	61.34	62.62	63.21	0.95
TiO_2	0.13	0.00	0.78	0.22	0.27	0.95	1.08	0.99	0.06	0.43	0.00
Al_2O_3	11.10	0.00	15.49	16.52	15.11	15.96	15.60	15.96	13.09	16.82	–
FeO	11.34	0.00	3.71	4.30	2.18	3.09	5.04	2.92	3.68	2.24	0.94
MnO	0.12	0.06	0.08	0.11	0.13	0.07	0.11	0.11	0.12	0.10	–
MgO	5.65	0.04	2.23	0.71	1.53	0.90	3.07	2.00	2.79	1.63	–
CaO	6.80	56.80	6.74	6.79	5.71	5.34	3.19	2.84	4.89	2.54	30.61
BaO	0.00	0.01	0.04	0.03	0.00	0.07	0.08	0.18	0.03	0.00	0.60
SrO	0.01	0.12	0.31	0.11	0.17	0.00	0.00	0.00	0.00	0.07	1.76
Na_2O	0.45	0.02	2.58	2.06	3.81	3.37	2.98	4.67	5.18	3.60	5.03
K_2O	0.24	0.09	9.74	9.49	9.60	9.34	5.97	8.73	7.89	7.30	7.14
P_2O_5	0.03	0.03	0.00	0.00	0.00	0.00	0.08	0.05	0.01	0.00	1.23
Ce_2O_3	1.06	0.00	0.07	0.10	0.02	0.05	0.10	0.10	0.01	0.13	0.40
La_2O_3	0.16	0.05	0.01	0.03	0.09	0.04	0.01	0.01	0.00	0.01	0.13
ZrO_2	–	–	0.11	0.13	0.12	0.12	0.20	0.09	0.05	0.04	–
F	0.31	1.09	1.12	1.18	0.65	0.51	1.58	0.51	0.19	0.76	1.96
Cl	0.06	0.02	0.18	0.18	0.12	0.16	0.15	0.02	0.02	0.20	–
S	0.04	0.04	0.07	0.23	0.06	0.11	0.14	0.07	0.08	0.03	42.62
Total	92.00	60.42	99.92	100.10	99.50	98.98	100.71	100.59	100.71	99.09	93.37

Note: 1 and 2, daughter minerals: 1, amphibole (?) and 2, calcite; 3–11, glasses of homogenized melt inclusions. Sulfur content in analysis 11 is given in SO_3 form.

is a fluorapatite with high concentrations of REE (up to 1.3 wt % $Ce_2O_3 + La_2O_3$). It should be noted however that, in addition to apatite, garnet contains a mineral of the phosphate class having lower (compared to apatite) concentrations of P_2O_5 (16–23 wt %) and high concentrations of SiO_2 (up to 10 wt %), Ce_2O_3 (5–7 wt %), La_2O_3 (3 wt %), S (up to 3 wt %), ThO_2 (up to 2.5 wt %), Nd_2O_3 (up to 1.7 wt %), and Sm_2O_3 (up to 1 wt %). This phosphate mineral is transitional in composition between apatite and britholite. Calcite in crystalline inclusions contains up to 0.8 wt % FeO.

The sulfate minerals of inclusions are represented by gypsum in garnet and celestite in sphene. These inclusions are nearly oval in shape and their average size is 20–30 μm. The difference between the analysis total and 100% suggests that the gypsum contains about 10 wt % H_2O. It is rich in SrO (up to 1.5 wt %). Celestite contains an admixture of BaO (no more than 1.2 wt %).

Among the salt minerals occurring as individual crystalline phases, fluorite should be noted. It occurs as light violet crystals, up to 30 μm in size, in potassium feldspar in association with silicate crystalline inclusions. The fluorite is poor in REE (Ce and La), and its total REE content is no higher than 0.05 wt %.

Thus, the established association of crystalline inclusions almost exactly mirrors the modal composition of the rock and confirms the possibility of their crystallization from a magmatic melt.

Melt Inclusions

Primary melt inclusions were found in the main rock-forming minerals, diopside, potassium feldspar, garnet, and sphene. They are represented by silicate (in diopside, sphene, and potassium feldspar) and salt melts (in diopside and garnet). In addition, garnet bears combined silicate–salt inclusions. All the inclusions are well crystallized, show no preference for particular mineral zones, and have sizes of 20–50 μm. The chemical compositions of daughter minerals from melt inclusions and homogenized glasses of these inclusions are shown in Tables 3–6.

Silicate and salt melt inclusions were found in **diopside**. Some growth zones of diopside crystals contain inclusions of both types, which suggests that they are cogenetic. All the inclusions have irregular shapes with

Table 4. Chemical compositions (wt %) of the glasses of homogenized melt inclusions in sphene and potassium feldspar from the garnet-bearing syenite porphyry

Component	1	2	3	4	5	6	7	8	9	10	11	12	13
SiO_2	64.68	64.65	63.20	63.48	63.06	63.65	66.02	63.98	65.76	66.37	62.34	63.78	63.91
TiO_2	0.66	0.85	0.50	1.48	2.59	2.80	0.53	0.83	1.18	1.43	0.92	0.17	0.06
Al_2O_3	18.46	19.54	18.38	15.83	15.12	15.40	18.88	17.93	17.32	18.10	17.97	18.17	17.90
FeO	0.31	0.12	0.22	2.46	2.62	2.72	0.12	1.06	0.14	1.39	0.23	3.20	2.83
MnO	0.00	0.00	0.00	0.06	0.10	0.12	0.07	0.05	0.01	0.06	0.00	0.06	0.00
MgO	0.03	0.04	0.03	0.08	0.06	0.08	0.04	0.05	0.03	0.27	0.07	0.41	0.67
CaO	1.09	1.44	0.57	2.36	4.34	3.80	1.13	2.03	1.98	2.01	1.20	2.81	3.12
BaO	0.09	0.05	0.19	0.02	0.12	0.01	0.04	0.10	0.15	0.00	0.03	0.30	0.34
SrO	0.00	0.00	0.08	0.06	0.11	0.33	0.06	0.02	0.03	0.00	0.15	0.37	0.17
Na_2O	5.64	3.32	3.22	3.41	3.21	2.32	4.27	3.88	4.20	4.17	4.31	4.19	4.76
K_2O	9.74	8.04	13.85	6.38	6.23	6.02	7.80	7.84	6.69	6.24	9.79	7.33	7.31
P_2O_5	0.01	0.00	0.01	0.00	0.05	0.01	0.01	0.00	0.04	0.01	0.02	0.01	0.04
Ce_2O_3	0.04	0.05	0.05	0.11	0.21	0.00	0.00	0.12	0.12	0.10	0.58	0.14	0.16
La_2O_3	0.00	0.00	0.09	0.00	0.11	0.16	0.02	0.05	0.06	0.07	0.57	0.00	0.06
ZrO_2	0.32	0.20	0.08	0.17	0.53	0.46	0.16	0.13	0.40	0.85	0.32	0.08	0.13
F	0.13	0.51	0.28	0.42	0.59	0.37	0.25	0.25	0.49	0.95	0.75	0.02	0.28
Cl	0.05	0.14	0.04	0.16	0.14	0.05	0.00	0.07	0.09	0.04	0.03	0.02	0.00
S	0.03	0.06	0.09	0.12	0.15	0.19	0.04	0.78	0.04	0.03	0.05	0.03	0.02
Total	101.27	99.01	100.88	96.58	99.32	98.49	99.43	99.15	98.74	100.13	96.88	101.09	101.76

Note: Glasses of homogenized melt inclusions: 1–11, in sphene and 12–13, in potassium feldspar.

uneven boundaries, and their gas phase is not clearly discernible. The inclusions are filled with a mineral aggregate composed of isotropic and anisotropic phases. Among the crystalline phases of silicate inclusions, an amphibole-like mineral, mica, and calcite were analyzed (Table 3). The daughter minerals of the salt inclusions were not identified because of the small sizes of individual grains.

The melting of phases in the silicate inclusions was first observed at a temperature of 840°C, when the gas phase took on a regular spherical shape. The last solid phase was resorbed in the inclusions at 950–970°C. The complete homogenization of silicate inclusions was attained at temperatures of 1010–1080°C. The homogenization temperatures of salt inclusions in diopside are 1060–1080°C.

Melt inclusions in **sphene** and **potassium feldspar** have negative crystal shapes and are 10 to 40 μm in size. Similar to the diopside-hosted inclusions, these inclusions are composed of fine-grained aggregates of isotropic and anisotropic daughter crystals, which prevented their analysis by a microprobe. The melt inclusions in sphene were completely homogenized at temperatures of 1010–1030°C, and those in potassium feldspar, at 1040°C.

Primary melt inclusions are most abundant in **garnets**. Salt melt inclusions and combined silicate–salt inclusions were distinguished among them. The salt melt inclusions were randomly distributed throughout the volume of crystals and some grains contain dozens of such inclusions. The inclusions have sizes of 20–50 μm and are usually irregular, occasionally rounded and partly faceted in shape. The combined silicate–salt inclusions are much rarer. They are usually irregular or rounded in shape, occasionally tubular. Their size varies from 40 to 25 × 60 μm.

The material of salt inclusions is holocrystalline, the gas phase is deformed and poorly discernible (Fig. 1a). Fluorite and calcite were reliably established among the phases of the inclusions (Table 5, an. 3). In addition, a Na–Ca sulfate phase was detected among the daughter minerals of melt inclusions (Table 5, an. 1, 2). This phase occupies a significant portion of the inclusion volume and was previously found by us as a daughter mineral of fluoride–sulfate and chloride–sulfate inclusions in fluorite from the celestite–fluorite ore of the Mushugai-Khuduk complex [8]. A remarkable feature of the Na–Ca sulfate phase is its enrichment in F (1.8–3.5 wt %). Furthermore, the analytical totals of this phase are much lower than 100%, which is probably

Table 5. Chemical compositions (wt %) of the daughter minerals and glasses of homogenized salt melt inclusions in garnet from the garnet-bearing syenite porphyry

Component	1	2	3	4	5	6	7	8	9
CaO	35.62	45.02	58.51	32.95	32.47	31.35	34.40	34.10	39.42
Na_2O	8.50	3.04	0.02	4.70	2.88	5.55	3.02	2.50	3.02
K_2O	0.20	0.63	0.00	4.25	3.73	3.43	3.11	4.63	3.09
BaO	0.04	0.00	0.05	0.60	0.99	0.09	1.26	0.59	1.48
SrO	0.50	0.87	0.09	1.72	2.23	1.50	1.59	1.95	3.73
SO_3	38.90	37.27	0.05	40.42	45.67	42.30	38.77	39.47	31.22
F	1.81	3.45	0.00	1.88	3.21	1.68	3.81	1.16	4.62
Cl	0.27	0.41	0.02	1.01	1.22	1.02	0.63	1.19	0.84
SiO_2	0.51	0.30	0.47	0.64	0.52	0.39	0.52	0.52	1.29
TiO_2	0.01	0.06	0.03	0.05	0.05	0.02	0.00	0.03	0.21
Al_2O_3	0.17	0.12	0.24	0.15	0.19	0.14	0.44	0.09	0.35
FeO	0.46	0.37	0.42	0.44	0.45	0.44	0.67	0.36	0.75
MnO	0.09	0.05	0.00	0.05	0.06	0.03	0.11	0.05	0.01
MgO	0.00	0.03	0.00	0.21	0.17	0.00	0.28	0.23	0.15
P_2O_5	0.00	0.00	0.00	0.56	0.36	0.37	0.34	0.47	0.35
Ce_2O_3	0.00	0.02	0.00	0.20	0.35	0.21	0.48	0.22	0.46
La_2O_3	0.00	0.03	0.04	0.00	0.02	0.02	0.08	0.10	0.07
Total	87.08	91.65	59.94	89.83	94.57	88.54	89.51	87.66	91.07

Note: 1–3, daughter minerals of melt inclusions: 1 and 2, Na–Ca sulfate; 3, calcite; 4–9, glasses of homogenized melt inclusions.

due to the presence of water in its composition. This is indirectly supported by its unstable behavior under an electron beam. Observations of the behavior of these inclusions during thermometric experiments on the microscopic heating stage revealed the following changes in their phase composition. Evidence for the beginning of melting in the inclusions was documented at 570°C, and the gas phase formed a regular spherical bubble at 650°C. The melting of solid phases was completed at temperatures of 930–940°C, after which the inclusions contained only melt and gas phases. The salt melt was completely homogenized at a temperature of 1050–1070°C. The gas phase was observed to reappear during cooling at a temperature of 930–910°C, and further cooling produced a fine-grained aggregate within the inclusions.

The same inclusions were annealed in the electric furnace at a certain temperature and then quenched quickly (within 1–2 s). These experiments gave surprising results. Salt melt inclusions are usually quenched into an aggregate of crystal phases even at a rapid temperature decrease after complete homogeni-

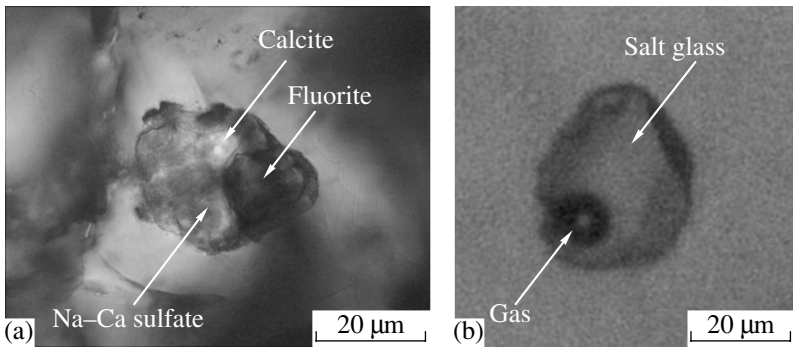

Fig. 1. Inclusions of sulfate melt in garnet from the garnet syenite porphyry. (a) Initial inclusion before heating and (b) inclusion after a thermometric experiment at 950°C and 1 atm.

Table 6. Chemical compositions (wt %) of the daughter minerals of combined silicate–salt melt inclusions in garnet from the garnet-bearing syenite porphyry

Component	1	2	3	4	5	6	7	8	9	10	11
SiO_2	65.89	65.72	37.66	2.72	2.12	2.32	8.42	0.86	0.17	0.96	0.30
TiO_2	0.01	0.02	0.29	0.02	0.00	0.04	0.00	0.04	0.07	0.01	0.06
Al_2O_3	19.55	21.27	21.61	0.19	0.02	0.17	0.19	0.10	0.04	0.11	0.12
FeO	0.29	0.27	1.78	0.30	0.14	0.80	0.63	0.69	0.17	1.36	0.37
MnO	0.00	0.02	0.19	0.00	0.00	0.03	0.02	0.00	0.00	1.30	0.05
MgO	0.01	0.02	0.03	0.04	0.02	0.00	0.00	0.00	0.00	0.65	0.03
CaO	0.50	0.86	39.68	51.54	51.55	46.21	47.50	10.85	61.71	62.70	45.02
BaO	0.07	0.00	0.01	0.11	0.01	0.01	0.08	0.06	0.00	0.00	0.00
SrO	0.00	0.00	0.00	0.00	0.00	0.26	0.23	2.21	0.08	0.10	0.87
Na_2O	0.62	10.18	0.05	0.12	0.16	0.02	0.19	0.02	0.00	0.05	3.04
K_2O	13.19	0.19	0.00	0.03	0.01	0.02	0.03	0.00	0.00	0.11	0.63
P_2O_5	0.00	0.02	0.00	38.41	37.92	37.08	26.57	29.49	0.00	0.04	0.41
Ce_2O_3	–	–	–	2.20	2.57	7.56	6.11	20.75	–	–	0.02
La_2O_3	–	–	–	0.82	0.97	3.56	2.74	9.28	–	–	0.03
F	–	–	–	2.78	2.79	3.24	2.90	3.40	–	–	3.45
Cl	0.00	0.01	0.01	0.03	0.04	0.00	0.03	0.00	0.02	0.00	0.41
S	0.00	0.01	0.00	0.12	0.35	0.45	1.53	1.28	0.00	0.13	37.27*
Total	100.13	98.59	101.31	99.43	98.67	101.77	97.17	97.81	62.26	67.52	97.16

Note: 1–11, daughter minerals: 1, potassium feldspar; 2, albite; 3, grossular; 4–6, apatite; 7, phosphate; 8, phosphate (monazite?), total includes 13.39 wt % ThO_2, 0.45 wt % UO_2, 5.61 wt % Nd_2O_3, and 1.33 wt % Sm_2O_3; 9 and 10, calcite; and 11, sulfate.

*Concentration of SO_3.

zation. The inclusions in garnet and diopside quenched to homogeneous glasses after heating up to 930–950°C (Fig. 1b). The formation of carbonate and carbonate–phosphate glasses is a very unusual phenomenon and was experimentally reproduced only twice in the carbonate–phosphate–peridotite [17] and $CaCO_3$–$Ca(OH)_2$–CaF_2–$BaSO_4$–$La(OH)_3$ systems [18].

The silicate–salt inclusions (Table 6) are characterized by the occurrence of a garnet rim on the walls of vacuoles accounting for no more than 5 vol %. The composition of garnet in the inclusions corresponds to a grossular. In addition to garnet, the silicate mineral assemblage of the inclusions contains potassium feldspar and albite. The salt phases include a sulfate mineral close to gypsum in composition, calcite, and several phosphate minerals. The latter include (1) apatite; (2) a mineral transitional between apatite and britholite, which was also found among crystalline inclusions in garnet; and (3) a phase chemically similar to monazite. Apatite proper has the composition of fluorapatite (up to 3.3 wt % F) and contains 3.6–11 wt % REE (Ce_2O_3 + La_2O_3) and up to 0.45 wt % S. The phase transitional between apatite and britholite (Table 6, an. 7) is also rich in REE (Ce_2O_3 + La_2O_3), S (up to 1.5 wt %), and SiO_2 (8.4 wt %). The monazite-like mineral contains 30 wt % Ce_2O_3 + La_2O_3, 13.4 wt % ThO_2, 5.6 wt % Nd_2O_3, 1.33 wt % Sm_2O_3, and 0.45 wt % UO_2. These inclusions were not homogenized during thermometric experiments.

Thus, the thermometric investigations of melt inclusions in the minerals of the garnet syenite porphyry suggested that the phenocrysts of this rock crystallized at temperatures of 1080–1010°C.

Chemical Composition of Melt Inclusions

The analysis of glasses of homogenized melt inclusions in the rock-forming minerals of the rock studied led to the conclusion that its formation involved silicate (trapped in diopside, sphene, and potassium feldspar) and salt (trapped in diopside and garnet) melts.

Silicate melts. The SiO_2 content of homogenized melt inclusions in the minerals studied varies from 56 to 66 wt %, and the highest SiO_2 variations (56–63 wt %) were measured in clinopyroxene-hosted inclusions. A characteristic feature of all the melts trapped in diopside, sphene, and potassium feldspar is a very high alkali content. The concentration of Na_2O + K_2O in the melts is 9–17 wt %. The melts trapped in

Table 7. Calculated chemical compositions (wt %) of salt melts trapped as inclusions in the minerals of the Mushugai-Khuduk complex

Component	1	2	3	4
CaO	35.00	26.00	44.00	54.50
BaO	1.20	1.90	0.49	–
SrO	9.90	5.70	6.00	–
Na_2O	2.70	11.10	–	0.10
K_2O	3.90	3.70	–	–
SO_3	33.10	29.00	24.90	0.50
P_2O_5	–	–	17.00	17.60
F	5.50	2.10	3.71	1.80
Cl	0.10	10.90	0.05	–
CO_2	2.10	4.50	1.92	19.70
H_2O	6.00	4.70	–	–
SiO_2	–	–	0.46	0.80
TiO_2	–	–	–	–
Al_2O_3	–	–	–	–
FeO	–	–	0.48	2.60
MgO	–	–	–	–
Ce_2O_3	0.20	0.10	0.68	1.70
La_2O_3	0.30	0.30	0.31	0.70
Total	100.00	100.00	100.00	100.00

Note: 1, fluoride–sulfate melt; 2, chloride–sulfate melt; 3, phosphate–sulfate melt; and 4, phosphate–carbonate melt.

diopside show a significant enrichment of K_2O over Na_2O, with $K_2O/Na_2O_3 \sim 3 : 1$.

The chemical compositions of glasses of homogenized melt inclusions have specific features in each of the aforementioned minerals. For instance, the homogenized melt inclusions in diopside are enriched in FeO (up to 6 wt %), CaO (3–7 wt %), and ZrO_2 (up to 0.2 wt %) compared to the average syenite composition. Also noteworthy is the abundance of volatile components in these melts, up to 1.6 wt % F and up to 0.2 wt % Cl.

Similar to melt inclusions in diopside, the melts trapped in sphene are strongly variable in SiO_2 and Al_2O_3 (62–66 and 15–19.5 wt %, respectively). In addition, they are relatively rich in FeO (up to 2.7 wt %), TiO_2 (up to 2.8 wt %), and CaO (3–7 wt %) and poor in MgO (0.03–0.08 wt %). Compared to the melts from clinopyroxene, the melts trapped in sphene are significantly enriched in ZrO_2 (up to 0.8 wt %), which is indicative of a higher degree of magma differentiation. The concentrations of volatile components (F and Cl) in the glasses of melt inclusions in sphene are also high (0.95 and 0.16 wt %, respectively) but somewhat lower than in the melt inclusions in clinopyroxene.

The compositions of glasses from the homogenized melt inclusions in potassium feldspar show high concentrations of FeO (3 wt %), CaO (3 wt %), BaO (0.3 wt %), and ZrO_2 (up to 0.13 wt %) and low TiO_2 (0.06–0.20 wt %) and MgO (0.4–0.7 wt %). The average SiO_2 and Al_2O_3 concentrations are 64 and 18 wt %, respectively. The concentrations of Cl in the melts are no higher than a few hundredths of a percent and F varies from a few hundredths to 0.3 wt %.

The compositions of silicate melts trapped in the diopside, sphene, and potassium feldspar of the garnet syenite porphyry fall mainly within the alkali syenite field in the $Na_2O + K_2O$–SiO_2 classification diagram.

Salt melts. Salt melt inclusions were found in two minerals, diopside and garnet. Salt and silicate melt inclusions may coexist in single diopside grains. The chemical compositions of the salt melts trapped in diopside and garnet are identical. Their major components are CaO and SO_3 (32–38 and 37–40 wt %, respectively). Such high concentrations of SO_3 in melt allowed us to define the composition as sulfate-dominated. Similar to the silicate melts, the salt melts are rich in alkalis (up to 8 wt %). There are also high concentrations of SrO (up to 3.7 wt %), BaO (up to 1.5 wt %), P_2O_5 (up to 1.2 wt %), F (up to 3.8 wt %), and Cl (up to 1.2 wt %). On the other hand, the low analytical totals of homogenized glasses in inclusions in both diopside and garnet are indicative of substantial amounts of H_2O and CO_2. This supposition is supported by the presence among the daughter minerals of considerable fractions of a hydrous sulfate phase and calcite. As was noted above, sulfate salt inclusions were first found by us in fluorite from the celestite–fluorite ore of the complex studied [8]. Thermometric experiments with these inclusions were performed in the microscopic heating stage allowing visual observation, and the cooling of inclusions after complete homogenization lasted 1–2 min. As a result, the salt melt inclusions consisted of quench crystals at ambient temperature. The compositions of the salt melts were estimated from the volume fractions of daughter minerals and their chemical analyses. The calculated composition of salt melt trapped in fluorite from the celestite–fluorite ore is similar to the compositions of glasses of the homogenized salt inclusions in diopside and garnet from the syenite porphyry both in major components and trace elements (Tables 3, 4, 7).

DISCUSSION

The ore-bearing garnet syenite porphyry that was found in the region of the Mushugai REE–apatite deposit is a peculiar rock, whose genesis remained ambiguous up to now. As was mentioned above, the mineral and chemical compositions of this rock resemble those of sviatonossite, which is considered by some researchers [13, 19] as an igneous rock formed through

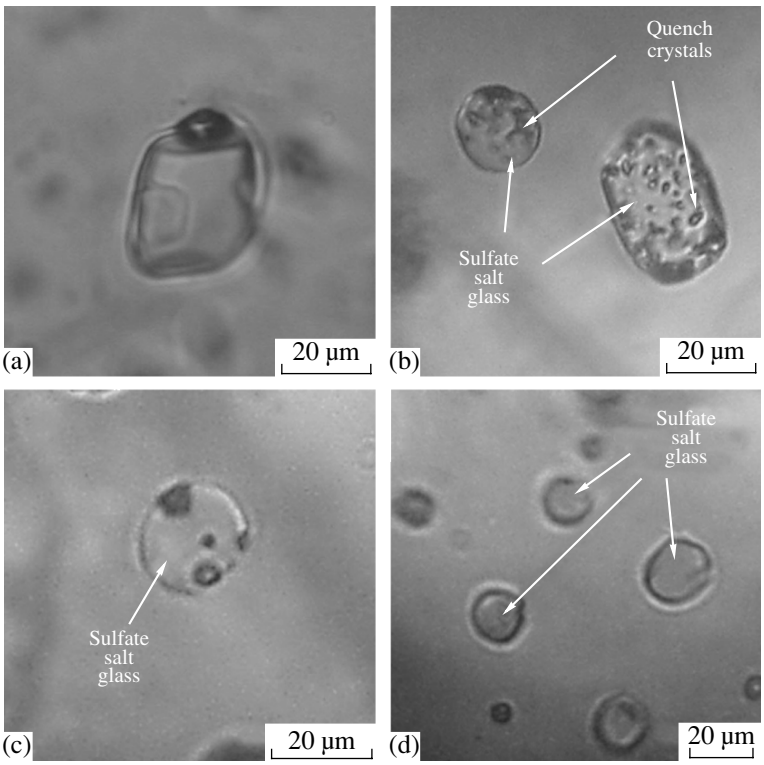

Fig. 2. Inclusions of sulfate melt in fluorite from the celestite–fluorite rock. (a) Initial inclusion before heating and (b)–(d) inclusions after thermometric experiments at 680°C and 1 atm.

the assimilation of limestones and products of their alteration by a syenite magma. A more popular hypothesis for the formation of sviatonossite involves high-temperature alkaline metasomatism of rocks of various initial compositions (basic rocks and syenites) in a calcium-rich environment [20–22].

Our investigations of melt inclusions in the minerals of the garnet syenite porphyry demonstrated that this rock crystallized from magmatic melts of silicate and salt compositions. One must remember that silicate melt inclusions were found in the phenocrysts of diopside, sphene, and potassium feldspar. The microprobe analysis of the homogenized glasses of these inclusions revealed widely varying SiO_2 concentrations ranging from 56 to 66 wt %. The glasses are characterized by very high concentrations of alkalis ($Na_2O + K_2O$ up to 17 wt %) and high contents of ZrO_2, F, and Cl. In general, the silicate melts are similar to the composition of alkali syenite.

Salt melt inclusions were found in diopside and garnet. All the salt melts have a sulfate-dominated composition with no more than 1.3 wt % SiO_2. The salt melts are also rich in alkalis, BaO, SrO, P_2O_5, F, and Cl. The salt inclusions in diopside associate with silicate melt inclusions, which suggests the coexistence of immiscible silicate and salt melts during the crystallization of this mineral. It should be noted however that pure silicate melt inclusions were never found in garnet.

Nonetheless, there are several lines of evidence that, similar to diopside, the garnet of this rock crystallized in equilibrium with silicate and salt melts. Among them are the occurrence of combined silicate–salt inclusions in garnet, the presence of cogenetic silicate and salt inclusions in single diopside grains, the similar homogenization temperatures of silicate and salt melt inclusions in diopside and salt inclusions in garnet, and the identical compositions of salt melt inclusions in the two minerals. The mechanism of selective entrapment of one of two coexisting liquids by minerals is not yet understood. However, such phenomena were reported in some studies [23, 24].

A peculiar result of our investigations of salt inclusions in garnet and diopside is the formation of homogeneous quench glasses in thermometric experiments, which provided a unique opportunity to precisely determine the composition of the salt melt. As was mentioned above, salt melts of similar compositions (fluoride–sulfate and chloride–sulfate) were found by us in fluorite from the celestite–fluorite ores of the Mushugai-Khuduk complex [8]. The homogenization experiments with the inclusions in fluorite were performed in a microscopic heating stage allowing visual observation. The relatively slow cooling (about two minutes) resulted in the formation of a fine-grained aggregate of quench crystals within those inclusions. The composi-

tion of the salt melt was therefore estimated by calculations. Keeping in mind that the salt inclusions in garnet and diopside from the garnet syenite porphyry yielded homogeneous glasses after experiments in the electric furnace allowing rapid quenching (1–2 s), we repeated homogenization experiments with the sulfate inclusions in fluorite from the celestite–fluorite rocks using the same procedure. Our previous experiments established homogenization temperatures of 600–670°C for the inclusions in fluorite, and new thermometric experiments were conducted under the same temperatures. After quenching the inclusions showed varying phase composition. The largest inclusions (30–40 μm) were composed of crystalline quench aggregates, whereas small inclusions (up to 20 μm) usually contained glass and quench microlites and, occasionally, homogeneous glass (Fig. 2). These observations allowed us to conclude that salt melts of such compositions can be quenched to glass under certain conditions.

The experimental study by Jones and Wyllie [18] of the multicomponent system $CaCO_3$–$Ca(OH)_2$–CaF_2–$BaSO_4$–$La(OH)_3$ containing 31.2 wt % $CaCO_3$, 24.9 wt % $Ca(OH)_2$, 13.5 wt % CaF, 10.4 wt % $BaSO_4$, and 20 wt % $La(OH)_3$ confirmed the possibility of the formation of salt glasses. These authors obtained carbonate-dominated glasses of the following composition at temperatures of 650–543°C and a pressure of 1 kbar: 45.0 wt % CaO, 6.59 wt % BaO, 18.2 wt % La_2O_3, 3.08 wt % SO_3, and 6.2 wt % F (total without CO_2, H_2O, and O = F is 76.46 wt %). Since glass formation was never reported in similar systems without $BaSO_4$ and $La(OH)_3$, in which synthetic liquids were always quenched to crystalline aggregates, the authors conjectured that the main factor of glass formation is the presence in the system of La; Ba; and, probably, SO_4 in certain proportions. The glasses from sulfate inclusions in clinopyroxene and garnet of the syenite porphyry also showed high concentrations of BaO and SrO together comprising up to 5.5 wt %, and elevated concentrations of Ce and La (up to 0.5 wt %), although they are not so high as in the experimental carbonate glasses. Thus, it cannot be excluded that the formation of salt glass during the quenching of homogenized melt inclusions was primarily related to the influence of the aforementioned components and SO_4.

Variation diagrams of major and minor elements against SiO_2 for the glasses of homogenized melt inclusions display distinct trends in the behavior of some major and volatile components (Al_2O_3, FeO, CaO, ZrO_2, F, and Cl) during syenite melt evolution. The results are illustrated in Fig. 3. The diagram SiO_2–Al_2O_3 exhibits an increase in the concentration of alumina in melts with increasing SiO_2, which is controlled by the crystal fractionation of primarily garnet and clinopyroxene, and, possibly, salt melt separation. The positive correlation between SiO_2 and ZrO_2 also suggests gradual zirconium accumulation in residual silicate melt in the course of magma evolution. The concentrations of ZrO_2 in the most evolved liquids are as high as 0.5–0.8 wt %.

Different tendencies were established for FeO, CaO, F, and Cl. The melts are depleted in these components with increasing SiO_2 content. The decrease in the FeO concentration in the melts was controlled by the extensive fractionation of garnet and clinopyroxene. The fractionation of these minerals was also responsible for the evolution trend in the CaO– SiO_2 diagram, whereas the role of apatite, calcite, and salt melt was subordinate. The significant depletion of melts in volatile components (F and Cl) with increasing SiO_2 concentration could be related primarily to the separation of salt melt already extracting these components from silicate melt during the early stages of syenite magma crystallization. On the other hand, the depletion of melt in F and Cl could be also related to fluorite and apatite fractionation.

A characteristic feature of all the melts studied, both silicate and salt, is their fluorine-rich compositions. The analysis of the behavior of various components as functions of fluorine concentration is therefore of particular interest. The diagrams of Fig. 4 show that the silicate melts tend to become depleted in alumina and alkalis and enriched in CaO and Cl with increasing fluorine concentration.

The compositions of salt melts show a distinct negative correlation between K_2O and F. The concentrations of Na_2O in the salt melts are not described by a single dependency and form two trends. One of them exhibits a strong enrichment of melt in Na_2O with increasing fluorine concentration, which could eventually result in the saturation of melt with respect to villiaumite. Kogarko [25] argued that an immiscible fluoride liquid saturated in NaF could be separated from alkaline melts during the late stages of the crystallization of agpaitic nepheline syenites. The second trend is defined by the salt melts showing an increase in Na_2O concentration at relatively constant fluorine concentrations. The trend of Cl versus F concentration is similar to that of Na_2O. There are again two groups of melts, one of which shows Cl accumulation with increasing F concentration, the other of which is characterized by a negative correlation between these components. The existence of two trends in salt melt composition is probably explained by the subsequent unmixing of the sulfate melt enriched in F and Cl into two liquids of fluoride–sulfate and chloride–sulfate compositions. Such melts were documented during our investigation of the celestite–fluorite ores of the Mushugai-Khuduk complex. This supposition is illustrated by the Na_2O–F diagram, where the points of the fluoride–sulfate and chloride–sulfate melts lie on the extensions of the two trends.

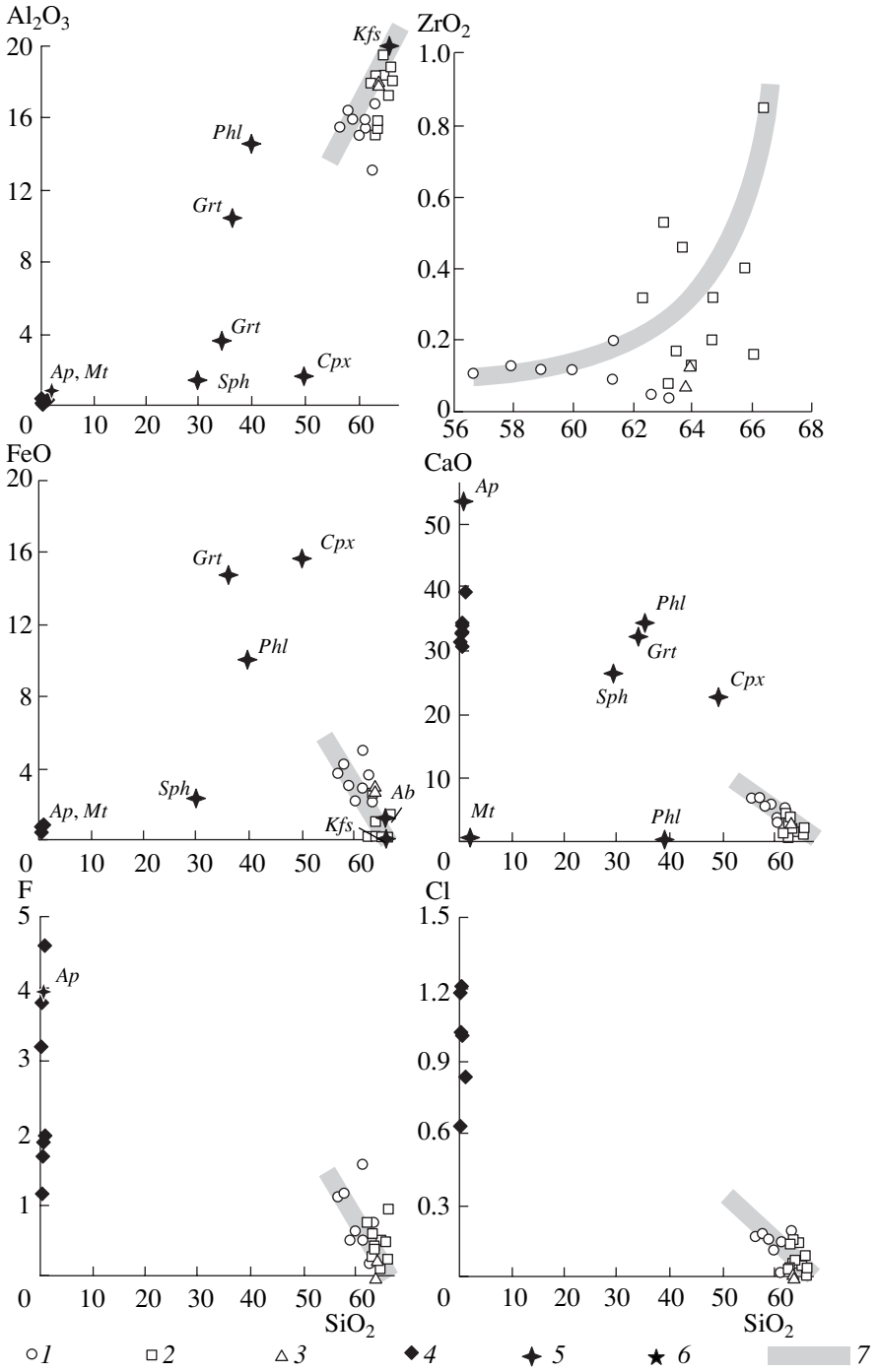

Fig. 3. Variations in the compositions (wt %) of melt inclusions in the minerals of the garnet syenite porphyry versus the SiO_2 concentration in the melt. (*1*)–(*4*) Melt inclusions in (*1*) clinopyroxene, (*2*) sphene, (*3*) potassium feldspar, and (*4*) garnet; (*5*) compositions of minerals: *Grt*, garnet; *Cpx*, clinopyroxene; *Phl*, phlogopite; *Kfs*, potassium feldspar; *Sph,* sphene; *Ap*, apatite; and *Mt,* magnetite; (*6*) calculated composition of salt melt trapped in fluorite of the celestite–fluorite rocks of the Mushugai-Khuduk complex; and (*7*) trends of melt evolution.

Of special interest is the behavior of REE in the silicate and salt melts. Figure 5 exhibits a strong positive correlation between Ce_2O_3 and F, which suggests that the degree of melt enrichment in cerium is a function of the fluorine content. The maximum concentrations of Ce_2O_3 (0.5 wt %) and F (4.6 wt %) were measured in the salt melts. This could lead to the crystallization of REE carbonates, fluorapatite, fluorite, and, probably, cerium fluoride (fluorcerite) from these liquids. This allows us to connect the genesis of REE-bearing carbonatites and various fluoride ores, which defined the metallogenic signature of the Mushugai-Khuduk complex, with the salt melts considered in this study.

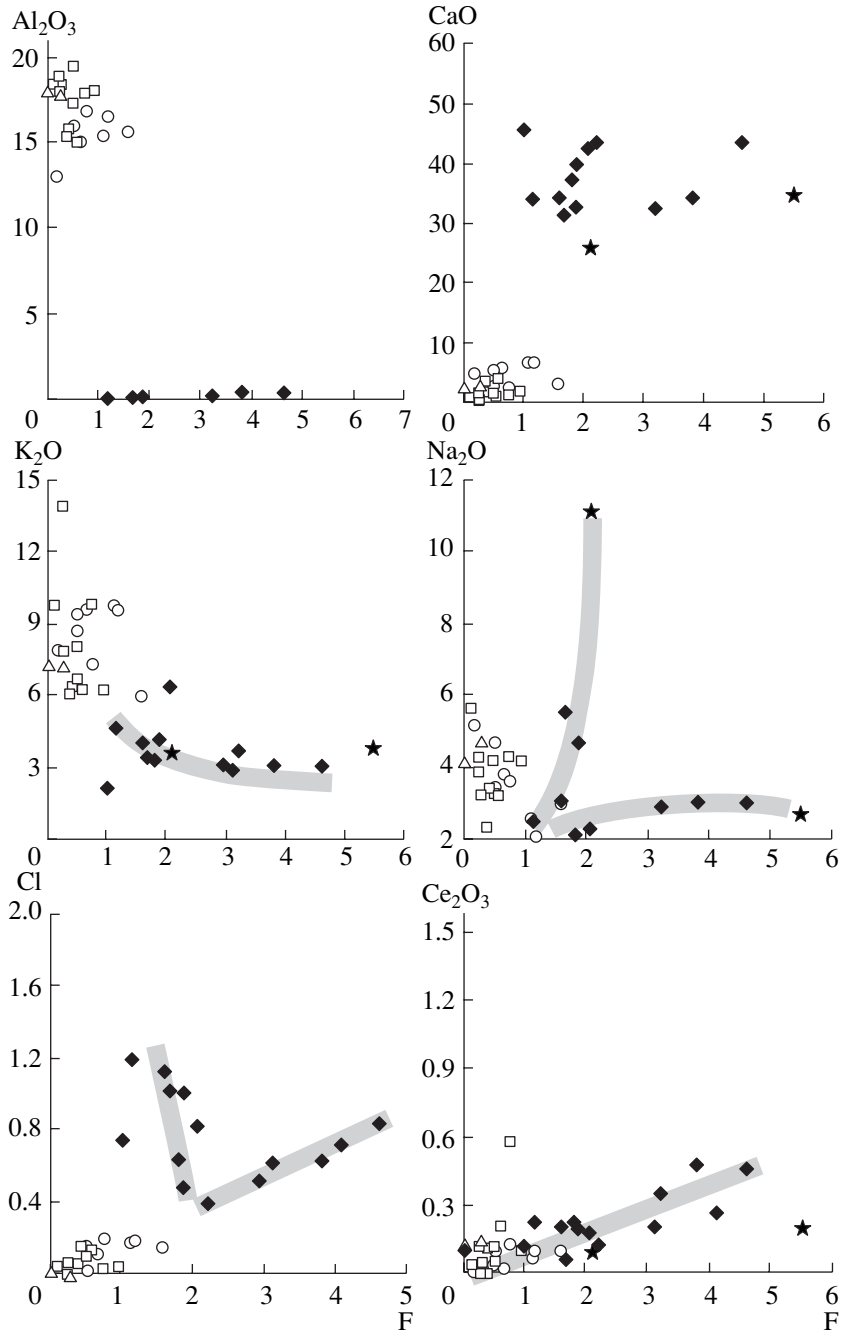

Fig. 4. Variations in the compositions (wt %) of melt inclusions in the minerals of the garnet syenite porphyry versus the F concentration in the melt. Symbols are the same as in Fig. 3.

Taking into account the sulfate-dominated chemistry of the salt melts, we examined the correlations between various components and the SO_3 concentrations. Figure 5 shows that the concentrations of CaO, SrO, Ce_2O_3, and F in the inclusions in general decrease with decreasing SO_3 content. Of particular importance is the behavior of Ce_2O_3 and F versus sulfur, which again highlights the key role of fluorine in the accumulation of REE in salt melts. On the other hand, there is considerable scatter in the concentrations of elements in the melts at a given SO_3 concentration. This scatter is probably related to the processes of liquid immiscibility.

Thus, the analysis of the behavior of silicate and salt melt compositions in the course of their evolution allowed us to conclude that the rock was formed under the influence of two main magmatic processes: crystallization differentiation and liquid immiscibility. The high concentrations of volatile components, in particular fluorine and chlorine, in the alkaline syenite magma probably played a leading role in the separation of salt

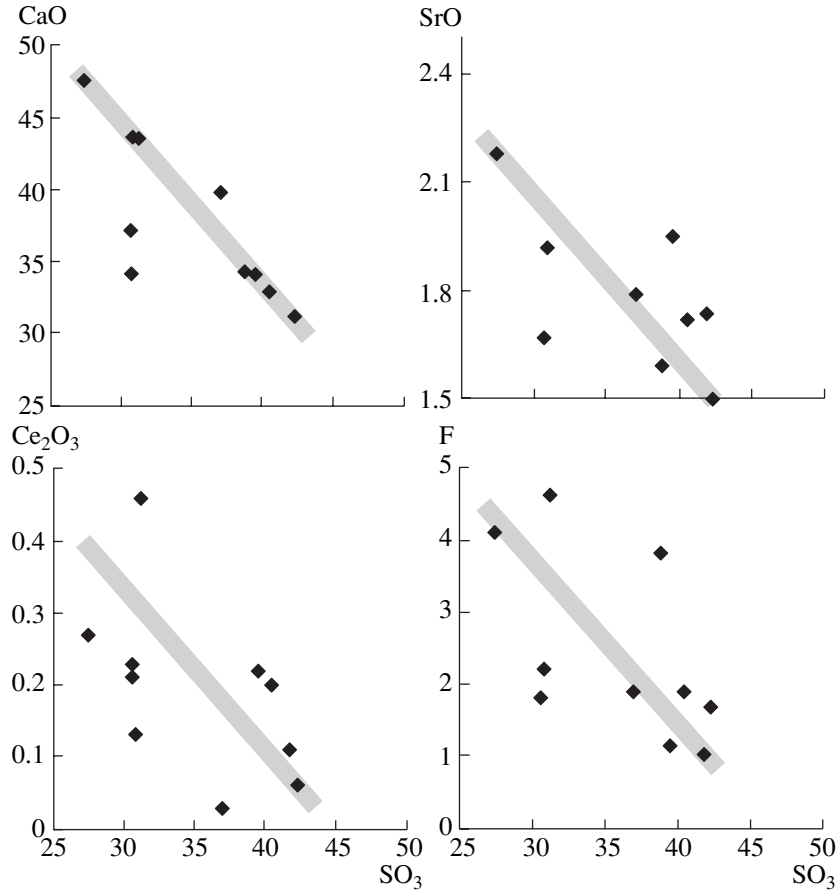

Fig. 5. Variations in the compositions (wt %) of melt inclusions in the minerals of the garnet syenite porphyry versus the SO_3 concentration in the melt. Symbols are the same as in Fig. 3.

melts. In addition to fluorine and chlorine, the salt melts extracted considerable amounts of calcium, alkalis, sulfur, phosphorus, trace elements (Ba and Sr), and rare earth elements (Ce).

CONCLUSIONS

(1) Crystalline and melt inclusions were found in diopside, sphene, potassium feldspar, and garnet from the garnet syenite porphyry of the carbonatite-bearing alkaline complex Mushugai-Khuduk. These results support the magmatic genesis of the rock. Magma crystallization occurred within a temperature interval of 1080– 1010°C.

(2) Silicate and salt melts were trapped as inclusions in the minerals of the syenite porphyry. Silicate melts were found in diopside, sphene, and potassium feldspar. They showed a wide range of SiO_2 concentrations, from 56 to 66 wt %, and high concentrations of alkalis (up to 17 wt % $Na_2O + K_2O$), ZrO_2, F, and Cl. In general, the silicate melts are similar in composition to alkaline syenite. Salt melt inclusions were found in diopside and garnet. Thermometric experiments with these melt inclusions produced homogeneous quench glasses of sulfate-dominated compositions with no more than 1.3 wt % SiO_2. The salt melts were very rich in alkalis, BaO, SrO, P_2O_5, F, and Cl.

(3) Our study demonstrated that fluorine played a leading role in the accumulation of light lanthanides, in particular Ce_2O_3, in sulfate salt melts.

(4) The investigation of the silicate and salt melt inclusions led us to the conclusion that the garnet syenite porphyry was formed under the influence of the processes of crystallization differentiation and magma unmixing into immiscible silicate and salt (sulfate) liquids.

ACKNOWLEDGMENTS

This study was financially supported by the Russian Foundation for Basic Research, project nos. 02-05-64190, 02-05-64191, and 01-05-64109; grant NSh 1145.2003.5 (Leading Scientific Schools); and project no. 00-05-72001 (Open Research Center for Mineral-Forming Media).

REFERENCES

1. L. N. Kogarko, Geol. Rudn. Mestorozhd. **41**, 387 (1999) [Geol. Ore Depos. **14**, 351 (1999)].
2. L. I. Panina, Geol. Geofiz. **38**, 112 (1997).
3. I. P. Solovova, A. V. Girnis, and I. D. Ryabchikov, Petrologiya **4**, 339 (1996) [Petrology **4**, 319 (1996)].
4. L. I. Panina and L. M. Usol'tseva, Petrologiya **7**, 653 (1999) [Petrology **7**, 610 (1999)].
5. I. P. Solovova, I. D. Ryabchikov, L. N. Kogarko, and N. N. Kononkova, Geokhimiya, No. 5, 435 (1998) [Geochem. Int. **36**, 377 (1998)].
6. I. A. Andreeva, V. B. Naumov, V. I. Kovalenko, and N. N. Kononkova, Dokl. Ross. Akad. Nauk **337**, 499 (1994).
7. I. A. Andreeva, V. B. Naumov, V. I. Kovalenko, and N. N. Kononkova, Dokl. Ross. Akad. Nauk **343**, 237 (1995).
8. I. A. Andreeva, V. B. Naumov, V. I. Kovalenko, and N. N. Kononkova, Petrologiya **6**, 307 (1998) [Petrology **6**, 284 (1998)].
9. I. A. Andreeva, V. B. Naumov, V. I. Kovalenko, and N. N. Kononkova, Geokhimiya, No. 8, 826 (1999) [Geochem. Int. **37**, 735 (1999)].
10. I. A. Andreeva, V. I. Kovalenko, and V. B. Naumov, Petrologiya **9**, 563 (2001) [Petrology **9**, 489 (2001)].
11. V. S. Samoĭlov and V. I. Kovalenko, *Complexes of Alkaline Rocks and Carbonatites in Mongolia* (Nauka, Moscow, 1983) [in Russian].
12. W. A. Deer, R. A. Howie, and J. Zussman, *Rock-Forming Minerals* (Longman, London, 1962; Mir, Moscow, 1965), Vol. 1.
13. P. Escola, Overs. Finska Vetensk. Soc. Forhandl. **13**, 1 (1921).
14. V. P. Chupin, D. V. Kuzmin, and J. L. R. Touret, in *Abstracts of XVI European Current Research on Fluid Inclusions, Porto* (Porto, 2001), p. 95.
15. A. V. Titov, S. V. Khromykh, A. G. Vladimirov, and L. N. Pospelova, Dokl. Ross. Akad. Nauk **377**, 86 (2001) [Dokl. Earth Sci. **377**, 229 (2001)].
16. L. I. Panina, A. M. Sazonov, and L. M. Usol'tseva, Geol. Geofiz. **42**, 1314 (2001).
17. I. D. Ryabchikov, G. P. Orlova, V. G. Senin, and N. V. Trubkin, Geol. Rudn. Mestorozhd., No. 3, 78 (1991).
18. A. P. Jones and P. J. Wyllie, Econ. Geol. **78**, 1721 (1983).
19. T. Sh. Tatevosyan, Izv. Akad. Nauk Arm. SSR, Geol. Geogr. Nauki **13** (5), 15 (1960).
20. O. A. Bogatikov, in *Alkaline Rocks of Siberia* (Nauka, Moscow, 1962), pp. 72–85 [in Russian].
21. V. A. Kononova, Izv. Akad. Nauk SSSR, Ser. Geol., No. 5, 37 (1957).
22. A. P. Ponomareva, Geol. Geofiz., No. 12, 51 (1989).
23. Roedder, E., *Fluid Inclusions,* Rev. Mineral. **12** (1984).
24. V. M. Kalugin, Candidate's Dissertation in Geology and Mineralogy (Moscow, 2002).
25. L. N. Kogarko, *Problems of the Genesis of Agpaitic Magmas* (Nauka, Moscow, 1977) [in Russian].